HTML ABSTRACT + LINKS

Effect of lattice-misfit strain on the process-induced imprint behavior in epitaxial $Pb(Zr_{0.52}Ti_{0.48})O_3$ thin films

Wenbin Wu[a)] and Y. Wang
Structure Research Laboratory, University of Science and Technology of China, Hefei 230026, China and Department of Applied Physics, The Hong Kong Polytechnic University, Hong Kong, China

G. K. H. Pang, K. H. Wong, and C. L. Choy
Department of Applied Physics, The Hong Kong Polytechnic University, Hong Kong, China

(Received 30 March 2004; accepted 1 July 2004)

The effect of lattice-misfit strain on the process-induced imprint behavior in $Pb(Zr_{0.52}Ti_{0.48})O_3$ (PZT) capacitors with Pt (top), and $SrRuO_3$, $La_{0.7}Sr_{0.3}MnO_3$ or $LaNiO_3$ (bottom) electrodes has been studied. With the different oxide electrodes and by changing the deposition oxygen pressure, various lattice-misfit strains in the epitaxial PZT films have been produced. It was found that after *in situ* annealing at reduced oxygen pressures, the capacitors showed an increased voltage offset in the polarization-electric field hysteresis loops with increasing the misfit strain, irrelevant to the oxide electrodes employed, while lattice disorder at the bottom interface can effectively eliminate the voltage shift. Our results suggest that the imprint behavior is caused by oxygen loss via dislocations generated by the misfit strain relaxation at the growth temperature. © *2004 American Institute of Physics*. [DOI: 10.1063/1.1786662]

Ferroelectric thin films possess a unique set of physical properties and have great potential for use in various electronic devices.[1] For successful implementation of ferroelectric devices based on polarization reversal, symmetric switching between two opposite polarization states must be ensured. However, it is often observed that ferroelectric films exhibit significant imprint, or asymmetry of switching parameters, such as the coercive field (E_c) and the remnant polarization (P_r).[2–10] The cause of the imprint is generally attributed to the presence of an internal electric field in the capacitor which supports the given polarization state while opposing the antiparallel one. However, there is a lack of understanding on the formation of the internal field. Different models, such as the aligned dipolar defect complexes and asymmetric distribution of charged defects through a bulk thin film,[2–5] and a built-in electric field or a nonswitching layer at the ferroelectric-electrode interface,[6–9] have been proposed to explain the asymmetric behavior of ferroelectric capacitors.

Pb(Zr,Ti)O_3 (PZT) and their derivatives are the most extensively studied ferroelectric materials due to their large P_r, low E_c and processing temperature. Since the PZT capacitors with noble metal electrodes like Pt exhibit a significant polarization loss when subject to bipolar switching pulses, in the past decade, for the growth of fatigue-free PZT capacitors and especially in the epitaxial form, various oxide electrodes such as $La_{0.5}Sr_{0.5}CoO_3$ (LSCO), $SrRuO_3$ (SRO), $La_{0.7}Sr_{0.3}MnO_3$ (LSMO), and $LaNiO_3$ (LNO) have been employed.[3–8,11,12] For epitaxial LSCO/PZT/LSCO capacitors, however, when exposed to reducing atmosphere for device fabrication, a large voltage offset was observed.[3–5] This process-induced imprint behavior was greatly complicated by the instability of the LSCO layer at reduced oxygen pressures,[5,13] and rarely examined for the other oxide electrodes. Comparatively, SRO, LSMO, and LNO are very stable and have different lattice constants.[14,15] Abe *et al.* demonstrated that the lattice-misfit strain is important for the voltage shift in epitaxial $BaTiO_3$ (BTO) film.[8] In this letter, the process-induced imprint behavior in epitaxial $Pb(Zr_{0.52}Ti_{0.48})O_3$ films on the SRO, LSMO, and LNO electrodes was studied, and by controlling the lattice constant of the bottom electrodes, the lattice-misfit strain effect was addressed.

The PZT/SRO(LSMO,LNO) heterostructures were grown on $(LaAlO_3)_{0.3}(SrAl_{0.5}Ta_{0.5}O_3)_{0.7}$ [LSAT(001)] substrates by the pulsed laser deposition method, as described previously.[11,15] All the films were grown at 640 °C with the deposition oxygen pressure fixed at 100 mTorr for SRO and LNO, and 200 mTorr for PZT. The LSMO electrodes were deposited at 100, 75, 60, or 30 mTorr, so that for the same LSMO different lattice constants can be achieved.[15] After deposition, the films were cooled to 550 °C in 10 Torr of O_2, and then *in situ* annealed at 10 or 10^{-5} Torr for 30 min before being cooled to room temperature (RT) in the same annealing ambient. To simplify the role of the different bottom electrodes, on each heterostructure Pt top electrode was deposited at RT using a shadow mask with holes of 0.2 mm in diameter. The thicknesses of Pt, PZT, and the bottom electrode were about 40, 400, and 200 nm, respectively. The polarization-electric field (P–E) hysteresis loops of the capacitors were measured at RT using a RT66A tester.

Figure 1 shows x-ray diffraction (XRD, Cu$K\alpha$ radiation) profiles from all the PZT capacitors *in situ* annealed in 10 Torr of O_2. The specular linear scans around the (002) reflections are shown in Fig. 1(a), and correspondingly the ω-scan rocking curves (RCs) on the PZT(002) reflections are shown in Fig. 1(b). In Fig. 1(a), curves *a*, *b*, and *c* are from those with SRO, LSMO, and LNO bottom electrode, respectively, where the electrodes were deposited at 100 mTorr. It is seen that the PZT(002) reflections are almost the same, and the reflections from the bottom electrodes locate at different Bragg angles, indicating an out-of-plane lattice constant of 3.936, 3.882, and 3.846 Å for the SRO, LSMO, and

[a)]Electronic mail: wuwb@ustc.edu.cn

 © 2004 American Institute of Physics
Downloaded 27 Jul 2011 to 158.132.161.52. Redistribution subject to AIP license or copyright; see http://apl.aip.org/about/rights_and_permissions

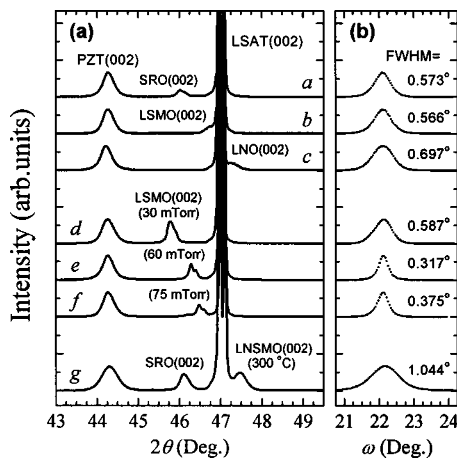

FIG. 1. (a) XRD specular linear scans around the (002) reflections of the various capacitors *in situ* annealed in 10 Torr of O_2. The curves *a*, *b*, *c*, *d*, *e*, *f*, and *g* are from the capacitor with SRO, LSMO, LNO, LSMO (30 mTorr), LSMO (60 mTorr), LSMO (75 mTorr), and LNSMO (300 °C) electrode, respectively. (b) XRD RCs on the PZT(002) reflections shown in (a). For clarity all the curves were shifted vertically.

LNO, respectively. These data imply that a full structural relaxation of each bottom electrode has been achieved. The RCs on the PZT(002) show that the PZT films are highly oriented, with the full width at half maximum (FWHM) of 0.5–0.7°. Curves *d*, *e*, and *f* are from the Pt/PZT/LSMO capacitors, where the LSMO films were deposited at 30, 60, or 75 mTorr. As has been pointed out, the oxygen content, and therefore the lattice constant of epitaxial $(La_{1-x}Nd_x)_{0.7}Sr_{0.3}MnO_3$ (LNSMO) films is quite sensitive to the deposition oxygen pressure at 10–100 mTorr, and is stable against *in situ* annealing in 10^{-6}–760 Torr of O_2.[15] This is true for the LSMO electrodes shown in Fig. 1. As the deposition oxygen pressure is decreased from 100 to 30 mTorr, the out-of-plane lattice constant was tuned from 3.882 to 3.961 Å. In Fig. 1(b), RCs on the PZT(002) reflections yielded a FWHM of 0.3°–0.6°. Further XRD off-specular scans on these capacitors were also performed and a parallel epitaxial relationship between the different oxide layers was confirmed. From these XRD data, an in-plane lattice constant of 3.886, 3.892, and 3.931 Å was calculated for the LSMO deposited in 75, 60, and 30 mTorr of O_2. For PZT, an in-plane lattice constant of 4.02 Å was also estimated after the reciprocal space mapping using Cu*K*α1 radiation.[16,17]

Figure 2(a)–2(c) show the *P*–*E* hysteresis loops recorded from capacitors *a*, *b*, and *c* as denoted in Fig. 1. The loops are symmetric for capacitor *a*, and slightly asymmetric for capacitors *b* and *c*. After *in situ* annealing at 10^{-5} Torr, as shown in Figs. 2(d)–2(f), only the LSMO and LNO electroded capacitors showed significant imprint. In both cases, the corresponding internal fields are directed toward the top electrode[4,10] and become larger as the lattice constant of the bottom electrode decreases. In order to understand the coercive voltage offset, and to make clear whether it is contributed by the built-in electric field at interface that may be different for the various electrodes,[6,7] the imprint behavior in PZT films on the same LSMO electrodes was investigated. As shown in Figs. 3(a)–3(c), after *in situ* annealing at 10 Torr, all the capacitors showed square *P*–*E* loops and a small voltage shift at the negative polarization state. After being treated in 10^{-5} Torr of O_2, as shown in Figs. 3(e) and

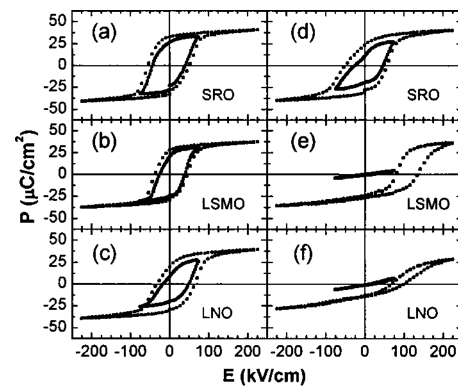

FIG. 2. *P*–*E* loops from the capacitors with different electrodes, as indicated. The loops in left (right) panels are from those annealed *in situ* in $10(10^{-5})$ Torr of O_2.

3(f), however, a large coercive voltage shift at the same state appeared. Also, the internal field increases as the LSMO lattice constant decreases. So the imprint seems to not result from the built-in electric field between PZT and the oxide electrodes. Instead, the lattice misfit strain in the PZT films, as a common feature, may cause the voltage shift observed.

Abe *et al.* have ascribed the voltage offset in epitaxial BTO films to the lattice-misfit strain at the BTO/SRO bottom interface. They assumed that at the interface a nonswitching layer exists, and it has a spontaneous polarization that cannot be switched by the applied voltage. In this layer the crystal structure may be asymmetrically deformed by relaxation of the lattice misfit strain.[8] Figure 4 shows transmission electron microscope (TEM) images of the PZT/LSMO interfaces with the LSMO layer deposited at 100 or 30 mTorr, as indicated. In Fig. 4(a), due to the large compressive misfit strain, a misfit dislocation network embodied by the periodically distributed bright spots was observed. As the lattice constant of LSMO increases, the misfit strain decreases,[16,17] and as a result, in Fig. 4(b) the spots disappeared. Figure 4(c) shows a high resolution image of the PZT/LSMO interface where the misfit dislocations and the lattice deformation of PZT were clearly observed. To further confirm that the lattice-misfit strain is critical for the imprint in epitaxial PZT films, we introduced lattice disorder at the PZT bottom interface by

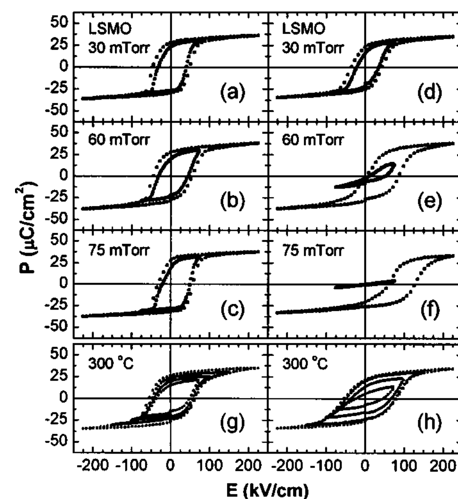

FIG. 3. *P*–*E* loops from the Pt/PZT/LSMO capacitors with the LSMO electrodes deposited at different conditions. The loops in the left (right) panels are from those annealed *in situ* in $10(10^{-5})$ Torr of O_2.

Downloaded 27 Jul 2011 to 158.132.161.52. Redistribution subject to AIP license or copyright; see http://apl.aip.org/about/rights_and_permissions

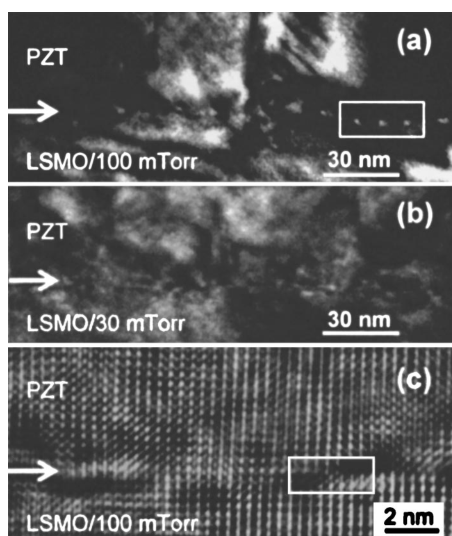

FIG. 4. Cross-sectional TEM images of the Pt/PZT/LSMO capacitors treated in 10 Torr of O_2. The LSMO electrode was deposited at 100 [(a) and (c)] or 30 mTorr (b). The white rectangles are guide to eyes for the misfit dislocations and the arrows are for the PZT/LSMO interfaces.

depositing a LNSMO ($x=0.5$) layer at a low temperature of 300 °C and in 100 mTorr of O_2 to reduce the misfit strain, although the Nd doping will decrease the lattice constant of LSMO further. To keep lower resistance of the bottom electrode, an epitaxial SRO film was first deposited at 640 °C. According to curve *g* in Fig. 1, the PZT(002) peak has broadened and correspondingly the RC showed a FWHM of 1.044°. The annealing effect on the *P–E* loops [Figs. 3(g) and 3(h)] showed that with the lattice disorder at the interface, the voltage shift has been effectively eliminated, as expected. After *in situ* annealing at 10^{-5} Torr, XRD results indicated that both PZT and the selected oxide electrodes are stable, with the same lattice constants recorded as for their counterpart treated in 10 Torr of O_2. Hence the oxygen loss may take place only at sites near the threading dislocations in the PZT layer which are normal to the film plane.[16,17] With the increase of lattice-misfit strain and thus the density of dislocations, a larger oxygen vacancy or stress related gradient near the bottom interface will be formed and along the out-of-plane direction, causing the larger internal field in the epitaxial PZT films.[4,10]

In summary, the lattice-misfit strain effect on the process-induced imprint behavior in epitaxial PZT films grown on SRO, LSMO, and LNO electrodes has been studied. It was found that after the reducing annealing, the PZT films showed an increased voltage shift with increasing the misfit strain. Our results suggest that an oxygen loss via misfit dislocations generated by the lattice-misfit strain relaxation may be responsible for the large voltage offsets.

This work was supported by the Chinese Natural Science Foundation, the Ministry of Science and Technology of China, and the The Hong Kong Polytechnic University.

[1] O. Auciello, J. F. Scott, and R. Ramesh, Phys. Today **51**, 22 (1998).
[2] D. Dimos, W. L. Warren, M. B. Sinclair, B. A. Tuttle, and R. W. Schwartz, J. Appl. Phys. **76**, 4305 (1994).
[3] G. E. Pike, W. L. Warren, D. Dimos, B. A. Tuttle, R. Ramesh, J. Lee, V. G. Keramidas, and J. T. Evans, Jr., Appl. Phys. Lett. **66**, 484 (1995).
[4] J. Lee and R. Ramesh, Appl. Phys. Lett. **68**, 484 (1996).
[5] T. Friessnegg, S. Aggarwal, R. Ramesh, B. Nielsen, E. H. Poindexter, and D. J. Keeble, Appl. Phys. Lett. **77**, 127 (2001).
[6] J. Lee, C. H. Choi, B. H. Park, T. W. Noh, and J. K. Lee, Appl. Phys. Lett. **72**, 3380 (1998).
[7] B. H. Park, T. W. Noh, J. Lee, C. Y. Kim, and W. Jo, Appl. Phys. Lett. **70**, 1101 (1997).
[8] K. Abe, N. Yanase, T. Yasumoto, and T. Kawakubo, J. Appl. Phys. **91**, 323 (2002).
[9] M. Grossmann, O. Lohse, D. Bolten, U. Boettger, T. Schneller, and R. Waser, J. Appl. Phys. **92**, 2680 (2002).
[10] A. Gruverman, B. J. Rodriguez, A. I. Kingon, R. J. Nemanich, A. K. Tagantsev, J. S. Cross, and M. Tsukada, Appl. Phys. Lett. **83**, 728 (2003).
[11] W. Wu, K. H. Wong, C. L. Choy, and Y. H. Zhang, Appl. Phys. Lett. **77**, 3441 (2000).
[12] M.-S. Chen, T.-B. Wu, and J.-M. Wu, Appl. Phys. Lett. **68**, 1430 (1996).
[13] S. Madhukar, S. Aggarwal, A. D. Dhote, R. Ramesh, A. Kishnan, D. Keeble, and E. Poindexter, J. Appl. Phys. **81**, 3543 (1997).
[14] M. Hiratani, C. Okazaki, K. Imagawa, and K. Takagi, Jpn. J. Appl. Phys., Part 1 **35**, 6212 (1996).
[15] W. Wu, K. H. Wong, X.-G. Li, C. L. Choy, and Y. H. Zhang, J. Appl. Phys. **87**, 3006 (2000); W. Wu, K. H. Wong, C. L. Mak, C. L. Choy, and Y. H. Zhang, *ibid.* **88**, 2068 (2000).
[16] C. M. Foster, W. Pompe, A. C. Daykin, and J. S. Speck, J. Appl. Phys. **79**, 1405 (1996).
[17] K. S. Lee, J. H. Choi, J. Y. Lee, and S. Baik, J. Appl. Phys. **90**, 4095 (2001).

Downloaded 27 Jul 2011 to 158.132.161.52. Redistribution subject to AIP license or copyright; see http://apl.aip.org/about/rights_and_permissions